University of Bristol - Explore Bristol Research
General rights

Research Article

Enhancing Radio Access Network Performance over LTE-A for Machine-to-Machine Communications under Massive Access

Fatemah Alsewaidi,[1] Angela Doufexi,[1] and Dritan Kaleshi[2]

[1]*Electrical and Electronic Engineering Department, University of Bristol, Bristol BS8 1UB, UK*
[2]*Digital Catapult, London NW1 2RA, UK*

Correspondence should be addressed to Fatemah Alsewaidi; eefaha@bristol.ac.uk, Angela Doufexi; a.doufexi@bristol.ac.uk, and Dritan Kaleshi; dritan.kaleshi@digicatapult.org.uk

The expected tremendous growth of machine-to-machine (M2M) devices will require solutions to improve random access channel (RACH) performance. Recent studies have shown that radio access network (RAN) performance is degraded under the high density of devices. In this paper, we propose three methods to enhance RAN performance for M2M communications over the LTE-A standard. The first method employs a different value for the physical RACH configuration index to increase random access opportunities. The second method addresses a heterogeneous network by using a number of picocells to increase resources and offload control traffic from the macro base station. The third method involves aggregation points and addresses their effect on RAN performance. Based on evaluation results, our methods improved RACH performance in terms of the access success probability and average access delay.

1. Introduction

Machine-to-machine (M2M) communication refers to data communication between entities (e.g., natural disaster alarms, smart meters, vehicle mobile global positioning systems (GPSs), and wearable health monitors) that do not necessarily need human interaction. Examples of M2M applications are shown in Figure 1. Different access-standardized technologies exist for M2M communications, such as wired networks (i.e., Ethernet), capillary (e.g., ZigBee and low-power WiFi), and cellular (e.g., General Packet Radio Service (GPRS) and Long Term Evolution-Advanced (LTE-A) standards). In this paper, we focus on the cellular M2M sector employing LTE-A technology. LTE-A provides benefits, such as ubiquitous coverage, large capacity, and interference management that enable it to cope with the needs of different M2M applications.

The general architecture of M2M communications over LTE networks and for M2M service requirements is described in [1–4]. Reference [5] introduces different network access methods for M2M devices (M2M-Ds). These methods are considered by the 3rd Generation Partnership Project (3GPP) in the description releases of the M2M work plan in [6]. M2M-Ds can directly establish a link with the evolved Node B (eNB) through an M2M gateway (M2M-GW) or with another M2M-D.

M2M communications will enable Internet of Things (IoT) connectivity. Advancements are swiftly moving from fourth-generation (4G) mobile communications toward ubiquitously connected devices. The increase of M2M-Ds is expected to reach 3.2 billion in 2019 [7]. 3GPP considered network enhancements for M2M communications in [4] and further optimization in LTE-A release 13 [8] for M2M communications that will enable LTE-A to play an essential role in fifth-generation (5G) systems.

Most M2M applications deal with infrequent small data transmissions. Nevertheless, this may cause network congestion, including radio access network (RAN) congestion, which affects network performance (such as by causing delays and reliability issues). This is especially the case if numerous devices access the network in a highly synchronized manner (e.g., after a power outage or violent windstorm). This leads to RAN congestion that causes an unacceptable delay, packet loss, or service unavailability [9]. The focus of this paper
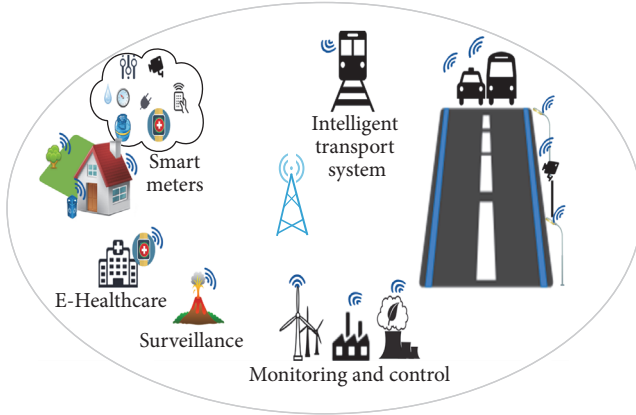
FIGURE 1: Examples of M2M applications.

is only on signalling congestion over RAN on account of the massive number of M2M-Ds simultaneously initiating a random access (RA) procedure.

A major research challenge in this context is development of an air interface to support the deployment of a massive number of M2M-Ds [10]. This paper addresses this challenge by investigating issues relating to RAN. These issues are highlighted below. In short, we

(i) simplify the complexity of the network to support the deployment of a massive number of M2M-Ds without influencing the LTE-A system architecture,

(ii) accommodate signalling overhead that is from a massive number of M2M-Ds,

(iii) achieve low latency, where some of the applications are nontolerant delay applications,

(iv) enhance the coverage for devices at the edge of the cell.

The major contributions of this paper are summarized below.

(i) We investigate the impact of the physical random access channel (PRACH) configuration index to increase random access opportunities (RAOs). The goal of this approach is to increase the number of RAOs and show how the increase affects RACH performance.

(ii) In addition, we examine the allocation of several pic-ocells to increase the number of preambles and decrease the traffic in the macrocell.

(iii) We furthermore consider employing aggregation points or M2M-GWs on the access points of small networks. In reality, we can find small networks within the range of a macrocell, but with different RAN technologies.

(iv) The goal of this approach is to explore the effect of aggregation points or M2M-GWs (aggregation points and M2M-GWs are hereafter interchangeably used) on RACH performance. The role of the aggregation

point is to collect device access requests from the small network and send them to the eNB and vice versa.

In this study, we aim to evaluate and enhance RACH performance over LTE-A under an extreme scenario (i.e., traffic model two in 3GPP [9]). In the extreme scenario, numerous M2M devices (up to 30,000) access the network over 10 s in a highly synchronized manner to enable implementation through beta distribution [9]. RACH performance is evaluated in terms of the preamble collision probability, average number of preamble transmissions, access success probability, and average access delay. The results are based on the unconditioned packet transmission [11, 12]. This study considers different density values according to [9] and statistics of available M2M-Ds in Bristol City Centre in the United Kingdom [13]. These values are used to analyse the RACH capacity. To validate the proposed approach, we built an RA procedure using MATLAB. The simulation results were validated in [13] with the 3GPP technical report [9].

The remainder of this paper is structured as follows. In Section 2, related work on existing RAN congestion control schemes is presented. The ways in which the proposed methods differ from those of previous works are also discussed. Section 3 overviews the contention-based RA procedure and RACH capacity evaluation metrics. RA improvement methods are outlined in Section 4. The system model and assumptions for the simulations are described in Section 5. An evaluation of RACH, including results and discussions, is presented in Section 6. Section 7 concludes this work.

2. Related Work

Various methods have been proposed to address the overload in RAN. General classification of these techniques based on [9, 10, 16–22] is shown in Figure 2. In [9], different solutions are proposed to control RAN congestion, including access class barring (ACB) schemes, separate RACH resources for M2M communications, dynamic allocation of RACH resources, slotted access, a specific backoff scheme, and a pull-based scheme. Those methods and others are likewise described in [17, 18]. In [23], the solutions proposed in [9] are evaluated for RACH overload (except slotted access and the pull-based scheme). Nonetheless, the mentioned methods are considered inefficient schemes if they are separately used [16].

In [24], the authors provided analysis that is applied to the RA procedure for M2M communications over LTE-A. The authors consider multiple classes with different qualities of service (QoS) for M2M-Ds in smart grids. The various classes are expressed by different ACB and backoff timers (BOs). They consider the on-off arrival process for M2M-Ds, which is a realistic approach for M2M communications in smart grid environments.

In [14], new mechanisms are proposed to solve RAN congestion considering only "delay tolerant" devices. The first method has a longer backoff value for preamble retransmission, which involves utilizing a longer backoff value in case of any collisions occurring to spread access reattempts from "delay tolerant" devices. The other method is the
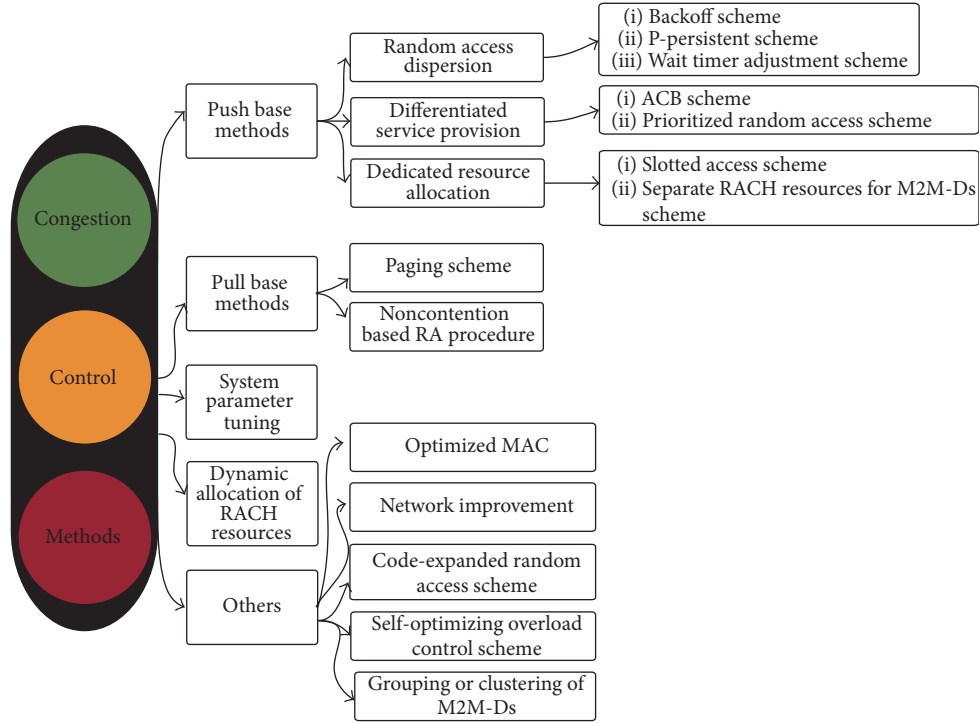
Figure 2: General classification of congestion control methods in RAN.

prebackoff approach undertaken before the first preamble transmissions, where the devices can read the random access response packet data unit (RAR PDU) of other devices to obtain the backoff information, even before performing the first attempt. This approach spreads the initial preamble transmission for a "delay-tolerant access" request over the timescale defined by the "delay tolerant access backoff value." The network can further prevent or spread the first preamble transmission with the prebackoff approach. Both methods have been evaluated under traffic model two with a maximum backoff value of 960 ms. The proposed schemes improve RACH performance in terms of access success, collision probability, and average preamble transmissions. However, no numerical results exist for the average access delay because they have only proposed solutions for "delay tolerant" devices. In [25], the authors proposed a dynamic backoff scheme to control the congestion in RAN. They evaluated the RACH performance, which considers extreme scenarios. This method enhances the access success probability; however, the drawback of this method is the increase of the access delay as a result of increasing the backoff timer. This increase is not accepted for nontolerant delay applications.

However, few studies consider the extreme scenario in which it generates synchronized traffic to evaluate RACH performance under the high density of devices within 10 s. The authors in [15] considered different traffic classes to address the RAN overload problem. They proposed the prioritized random access (PRA) architecture. The PRA architecture is comprised of two components: virtual resource allocation with class-dependent backoff procedures and dynamic access barring. They evaluated the RACH performance in terms of the access success probability and average access delay for each class. However, the average access delay for smart meters that arrived in a synchronized manner (i.e., the arrival rate follows the extreme scenario) is too high.

In [25], the authors proposed a dynamic backoff scheme to control the congestion in RAN. They evaluated the RACH performance with consideration of the extreme scenario. This method enhances the access success probability; nevertheless, it has the drawback of increasing the access delay as a result of increasing the BO. This increase is unacceptable for nontolerant delay applications. Meanwhile, the authors in [26] proposed a group-based optimization method with a resource coordination scheme in RACH. They classified the signalling messages into two types: diverse messages and redundant messages to avoid signalling congestion. Although this method enhances RACH performance in terms of access success probability, it provides no means to enhance RACH in terms of the access delay. Access delay is an important metric in the RACH performance evaluation and should therefore be considered.

In [27], a cooperative ACB scheme was proposed to enhance the performance of the ordinary ACB. This scheme is based on using the benefit of the heterogeneous multitier network in LTE-A. The authors deployed three picocells, each with 20% of the M2M-Ds among M devices, and seven macrocells with 6% of the M2M-Ds among M devices (i.e., except the centric macrocell with 4% of the M2M-Ds among M devices). Additionally, they jointly optimized the ACB parameters with all eNBs according to the level of congestion in each eNB. The scheme uses only one preamble to limit the random access resource to the time domain instead of

the preamble domain. The scheme improves the average access delay compared to the conventional ACB. However, the average access delay in the proposed scheme remains unacceptable because the average access delay for 30,000 M2M-Ds is approximately 4×10^4 ms. In addition, the authors did not indicate the type of traffic model used for the M2M-D arrival.

Recently, the authors in [28] provided a set of guidelines for the resource allocation task in RACH with an investigation on RACH performance in terms of the backoff timer and maximum preamble transmission attempt ($\text{Max}_{\text{PreamTrans}}$). However, traffic of the arrival devices follows a Poisson distribution, which is in contrast to the approach of this study. In [18], the effect of different settings of the PRACH configuration index (i.e., 0, 3, 6, and 9) was explored. Different values of $\text{Max}_{\text{PreamTrans}}$ (i.e., 3, 10, 15, and 50) increase the RA resources and chances for the devices to successfully access the network by increasing the attempts of, respectively, transmitting the preamble. The authors evaluated RACH performance under only simultaneous arrivals of more than 1,000 devices. The evaluation metrics used in [18] include the average access delay, average energy consumption, blocking probability, and average number of preamble transmissions. On the other hand, the focus of the present approach is traffic model two, whereby massive devices with different ranges (i.e., from 5,000 to 30,000 devices) synchronistically access the network within 10 s.

The authors in [13, 29] analysed RAN performance for 16,000 M2M-Ds for LTE-A in different frequency bands. The authors also considered tuning of different system parameters to enhance RACH performance, such as BO, the medium access control (MAC) contention resolution timer (*mac-Contention Resolution Timer*), and $\text{Max}_{\text{PreamTrans}}$. The results showed RACH enhancement in terms of the access success probability only for specific values of $\text{Max}_{\text{PreamTrans}}$. The BO was shown to improve RACH performance in terms of the access success probability; however, it increased the average access delay.

The motivation behind the approaches proposed in this paper is to address the congestion in RAN caused by signalling overhead using the existing LTE-A system architecture. In addition, this paper considers different densities of devices to evaluate RACH performance under extreme scenarios.

3. Random Access Channel

In LTE-A, M2M-Ds use the RA procedure to establish a radio link (i.e., creating a transition from the radio resource control (RRC) idle mode to the RRC connected mode) to complete an intrasystem handover for synchronizing the devices (in case they are in the RRC connected mode but not synchronized, and uplink or downlink data arrive). Alternatively, it synchronizes the devices to reestablish an RRC connection or to position or schedule a request. The RA procedure can be either contention-based or noncontention-based.

The contention-based RA procedure is used for connection establishment. The device randomly selects the access
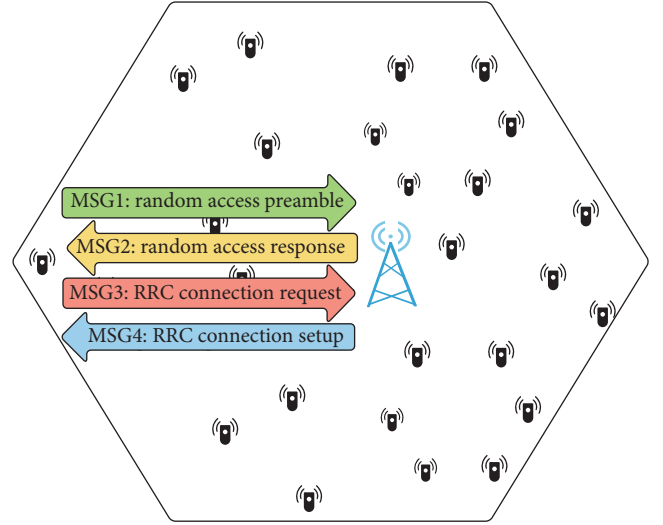

FIGURE 3: Contention-based RA procedure.

resources. On the other hand, the noncontention-based RA procedure is used for intrasystem handover and the arrival of the downlink data, where the access resources are assigned to the device by the eNB. In this study, our focus is on the contention-based approach, whereby the devices use the RA procedure to establish a radio link connection.

3.1. Contention-Based RA Procedure. As mentioned above, in our approach we use the contention-based RA procedure. It is a cross-layer procedure (i.e., MAC and physical layers) that deals with the logical, transport, and physical channels. The logical channels transfer data between the radio link control (RLC) and MAC sublayers (e.g., common control channel (CCCH)). The transport channels transfer data between the MAC and physical layers (e.g., RACH, downlink shared channel (DL-SCH), and uplink shared channel (UL-SCH)). However, the physical channels transfer data across the air interface (e.g., physical downlink control channel (PDCCH), PRACH, physical downlink shared channel (PDSCH), and physical uplink shared channel (PUSCH)).

The contention-based RA procedure messages pass through the mentioned channels. The contention RA procedure consists of four messages exchanged between the device and the eNB, as shown in Figure 3. RA procedure messages are described below.

(i) The first message (MSG1) is a random access preamble, whereby the device randomly selects a preamble out of 54 preambles, as assumed in [9], and sends the preamble to eNB. This message deals with RACH, which transfers the control information to PRACH. The device uses the transferred information to select a preamble and calculate the PRACH transmit power. It then transmits the preamble with a random access-radio network temporary identifier (RA-RNTI) on the PRACH to eNB in the next RAO. The RAOs are defined according to the PRACH configuration index, which is broadcasted within the system information

block two (SIB2). This step enables eNB to estimate the transmission time of the device to uplink the synchronization if there is no collision. A collision occurs if two or more devices send the same preamble to eNB in the same RAO, as defined in [9]. In this case, eNB will be unable to decode MSG1 from the collided devices; moreover, it will not respond to them with the random access response (RAR).

(ii) The second message (MSG2) is RAR, with which the eNB transmits the message to the device if there is no collision. This message includes a temporary cell-radio network temporary identifier (TC-RNTI) and a timing advance (TA) command (i.e., to adjust the device transmit timing). It assigns uplink resources to the device to be used in the third step. The device checks the PDCCH whose cyclic redundancy check (CRC) bits are scrambled by its RA-RNTI within the random access response window (RAR_{window}) to read the downlink control information (DCI) and obtain the downlink resource allocation information to identify the position of the RAR within the PDSCH. If the device does not find its PDCCH with its RA-RNTI, it means that either a collision occurred, as assumed in [9], or insufficient PDCCH resources are available.

(iii) The third message (MSG3) is an RRC connection request. Because we focus on the contention-based RA procedure for connection establishment, the device uses TC-RNTI to send the RRC connection request using signal radio bearer zero (SRB0) on CCCH. The data are then mapped onto UL-SCH, and uplink control information (UCI) is added to the outcome of the UL-SCH during physical layer processing for transfer to eNB using PUSCH. After sending MSG3, the device starts the contention resolution timer and awaits a response from eNB.

(iv) The fourth message (MSG4) is the RRC connection setup, wherein eNB sends MSG4 to the device using SRB0 on CCCH, which passes through DL-SCH using its TC-RNTI. The RRC connection setup message carries a cell-radio network temporary identifier (C-RNTI), which is used for further message exchange. The RA procedure is considered successful only if all steps are successfully completed. If the device does not receive a response within the *mac-Contention Resolution Timer*, then the device attempts to transmit a preamble again (but only if $Max_{PreamTrans}$ is not reached).

3.2. RACH Capacity Evaluation Metrics. The different measures that can be considered to evaluate the performance of RACH capacity for M2M communications are presented in a 3GPP report [9]. Here, we evaluate RACH by considering the collision probability under the unconditioned packet transmission. The knowledge of the collision probability is important for resource management.

The evaluation metrics used in this paper are the following [13]:

(i) Collision probability: the ratio of the number of occurrences in which a collision occurs to the overall number of opportunities (with or without access attempts) in the period.

(ii) Access success probability: the ratio between the number of devices successfully completing the RA procedure and the total number of devices.

(iii) Average access delay: the ratio between the total access delay time of the successful access devices and the time from the first RA procedure access to its successful completion when all devices successfully completed the RA procedure.

(iv) Average number of preamble transmissions: the ratio between the total number of preamble transmissions for all successful access devices and the total number of devices successfully completing the RA procedure within the maximum number of preamble transmissions.

4. Random Access Improvement Methods

As described above, we consider the contention-based RA procedure with a massive number of devices accessing the network within 10 s. This approach increases the contention on the RAOs and the PDCCH resources; moreover, it leads to a reduction of the access success probability. In [17], the authors indicated that RAN/core network (CN) resources are insufficient to meet the needs of all users and M2M-Ds. In this paper, we propose different methods to enhance RAN performance, as illustrated in Figure 4.

The first method increases the RAOs to increase the access resources by reconfiguring the PRACH configuration index. In the second method, we place several picocells in the macrocell range to increase PDCCH resources and reduce the traffic on eNB of the macrocell. In the last method, small networks are placed with aggregation points within the range of the macrocell. The evolution in 5G considers deploying aggregation points as one of the device access methods [30]. Those methods are presented in detail in the following subsections.

4.1. PRACH Configuration Index. The availability of RAOs relates to the PRACH configuration index. For example, if the configuration index is six, then there are two RAOs in each frame, as shown in Figure 5(a). By setting different values of this index, the availability of RAOs per frame changes. This fact has an intrinsic effect on the RACH performance. In Annex B of TR 37.868 by 3GPP, the RACH intensity is plotted against the required number of RAOs per second for a given collision probability of 1% [9]. They assumed that the arrival of RACH requests is uniformly distributed over time.

Meanwhile, the method in [18] uses 0, 3, 6, and 9 PRACH configuration index values to evaluate RACH performance of LTE with the assumption of fixing the initial number of simultaneous arrivals to a specific RA slot (i.e., RAO) without considering a traffic pattern for the simultaneous arrivals. The authors evaluate RACH with respect to the average access delay, blocking probability, average energy consumption, and
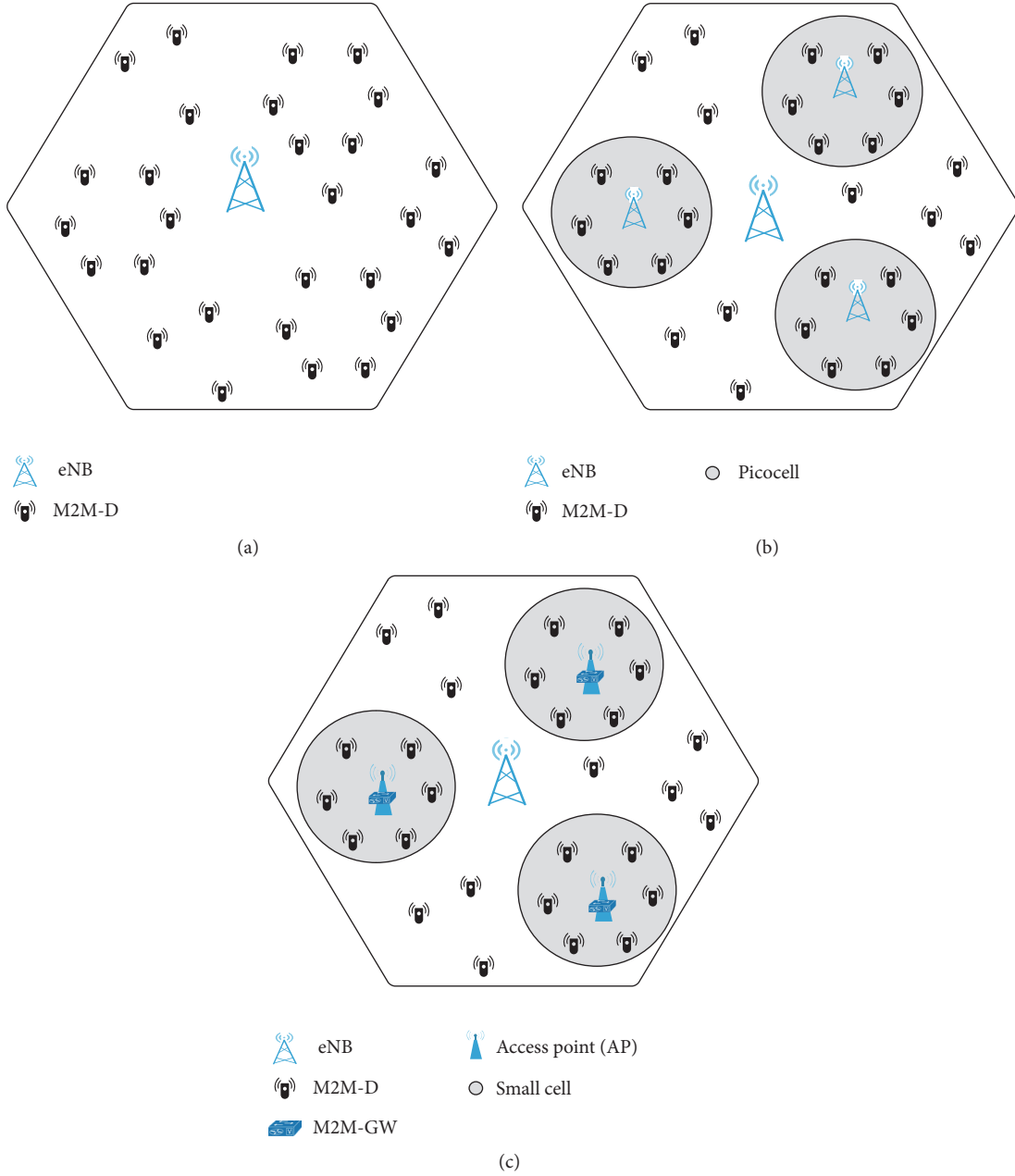
(a)

(b)

(c)

Figure 4: Proposed methods. (a) 3GPP scenario. (b) Picocells. (c) Aggregation points.

average number of preamble retransmissions. However, in this study, we investigate how the increase of RAOs affects the RACH capacity. Our study evaluates RACH performance under an extreme scenario (i.e., within 10 s), and the arrival of device access requests follow a beta distribution over time. To enhance RACH performance, we increase the RAOs per frame by setting the PRACH configuration index to 12. For this configuration, the availability of RAOs is five per frame, as shown in Figure 5(b).

4.2. Pico Cells. The primary role of heterogeneous networks is to provide more coverage and capacity (i.e., cover low-cost and low-power devices in coverage holes) [31]. For example,

a large cell is covered by a macro base station, where femto access points (FAPs), pico base stations (PBSs), or relay stations (RSs) are used for coverage extension and capacity growth.

Because the given network elements improve network performance in terms of capacity and coverage, an enhancement of RAN performance is also expected. Therefore, we chose PBS on account of its advantages over the other networks elements. Moreover, PBS uses less power and costs less compared to MBS. In addition, it is accessible to all cellular devices because it is part of a network operator that deploys the public infrastructure and is controlled by the network operator, which aids in further management.
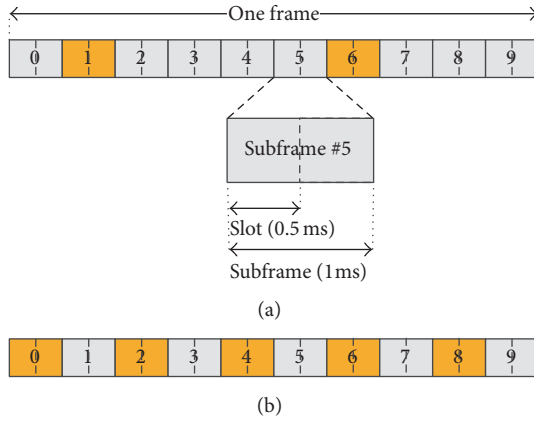
FIGURE 5: PRACH configuration index of frame structure type one. (a) PRACH configuration index six. (b) PRACH configuration index 12.

Furthermore, PBS transmissions are reliable and secure. In addition, placing PBSs in the area of MBS will increase access resources (i.e., preambles, PDCCH resources) that, in turn, will offload the traffic from the MBS to the PBSs, help to reduce MSG1 failures, and reduce the average access delay, especially in the case of many devices. Therefore, in our study, we place a different number of PBSs in the macrocell to improve RAN performance.

4.3. Aggregation Points. Involving aggregation points or M2M-GWs in an LTE-A system is being considered a solution to control RAN congestion in 5G systems [30]. It is also considered a radio access method for massive machine communications (MMC) [32]. The goal of using aggregation points is to provide interoperations with different wireless technologies [33]. In addition, deploying M2M-GW will help reduce device power consumption if it transmits through M2M-GW with low power [10].

In [5], an M2M-GW was introduced as an M2M-D access method to enable an efficient path for communication between devices. In [34], the authors proposed an architecture that supports the use of the M2M relay (M2M-R) as a data concentrator. The authors deployed an aggregation scheme in M2M-R, M2M-GW, and eNB. In addition, they proposed a possible design of M2M-GW in which the devices are linked to M2M-GW, which, in turn, is linked to eNB via an M2M-R. That study focused on data aggregation with a small number of devices (i.e., a maximum of 500 M2M-Ds). It showed a reduction in protocol overhead. In this paper, the aggregation point is used to gather the access requests of devices coming from the small network to which it belongs.

Two different scenarios for aggregation points are used for the access request under the extreme scenario (i.e., traffic model two in 3GPP [9]). In the first scenario, the aggregation point acts as a tunnel to pass device messages to and from eNB.

In the second scenario, we assume that the aggregation point is available for multipacket reception. The aggregation point has a behaviour that is similar to that of M2M-D in the RA procedure, whereby it shares the same access resources with M2M-Ds. The aggregation point collects device requests in each RAO and deals with the incoming requests as one request. The aggregator point refers to this request as a group request. Once the request of the group is granted, then the aggregation point grants the requests of the devices belonging to the same group. The devices in the granted group share the same uplink resources.

The aim of evaluating RAN performance in scenario one is to validate the implementation of aggregation points in our simulation for use in scenario two.

5. System Model and Assumptions

The system model accounts for the radio frame structure type one that is applicable to FDD. The M2M traffic arrival rate is assumed to follow a beta distribution (extreme scenario) with $\alpha = 3$ and $\beta = 4$. Under this scenario, numerous M2M-Ds attempt to access the network within 10 s in a highly synchronized manner [9]. A time domain random access structure of LTE is used. For statistically accurate results, an average of ten cells is deployed, each of which has a 1 km radius, which is taken as a typical size for a hexagon macrocell. The number of M2M-Ds in one macrocell is assumed to have the following values: 5,000, 10,000, 16,000, 20,000, 25,000, and 30,000.

The RA procedure was implemented using MATLAB. Our simulation results were validated in [13] with the 3GPP technical report [9]. The simulation parameters based on [9] are presented in Table 1.

We consider the limit of PDCCH resources that may cause an MSG2 failure. The RA configuration for the preamble format is zero, which will restrict the preamble length to 1 ms (T_{MSG1}). As mentioned in Section 3.1, the contention-based RA procedure has a total of 54 preambles ($N_{preamble}$). The use of PRACH configuration index six involves use of an RAO every half frame, as shown in Figure 5(a). Therefore, the total number of RAOs for the extreme scenario (over 10 s) is 2,000. Every activated device randomly sends a preamble (i.e., MSG1) within a maximum of ten preamble transmission attempts ($Max_{PreamTrans}$). Then, eNB processes MSG1 to check whether a preamble collision exists [9]. If there is no collision, eNB sends an RAR (i.e., MSG2) to the device within 3 ms (T_{MSG2}). Otherwise, the collided devices attempt access again after a period of time (i.e., T_{MSG2} + RAR$_{window}$ + the time uniformly selected by the device within BO) for a new RAO with a new preamble, as long as the number of preamble transmission attempts (i.e., Counter$_{PreamTrans}$) does not exceed $Max_{PreamTrans}$.

For simplicity, the ramping procedure, which is used to increase the power of the device after each retransmission, is implemented in this simulation as a function of $(1 - e^{-i})$ to describe the probability of a successful preamble transmission, where i represents the number of times the device transmits preambles (Counter$_{PreamTrans}$) [9]. The position of RAR for the granted devices is assigned through PDCCH within the RAR$_{window}$ [35]. It is assumed that in each RAR there are three uplink grants. The simulation assumes 16 common control elements (CCEs), where the aggregation level is four (i.e., the PDCCH format is two). Therefore, the

Table 1: Simulation parameters.

Symbol	Parameter	Value
B	Cell bandwidth	5 MHz
—	PRACH configuration index	6
$N_{preamble}$	Total number of preambles	54
$Max_{PreamTrans}$	Maximum number of preamble transmissions	10
—	Number of UL grants per RAR	3
—	Number of CCEs allocated for PDCCH	16
—	Number of CCEs per PDCCH	4
RAR_{window}	*RA-Response Window Size*	5 ms
—	*mac-Contention Resolution Timer*	48 ms
BO	Backoff timer	20 ms
—	Probability of successful delivery for both MSG3 and MSG4	90%
$MaxRetrans_{HARQ}$	Maximum number of HARQ transmissions for MSG3 and MSG4 (nonadaptive HARQ)	5
M	Number of MTC devices ($\times 10^3$)	5, 10, 16, 20, 25, 30
T_u	Number of available subframes over the distribution period	10,000
b	Periodicity of PRACH opportunities	5 ms
T_{MSG1}	MSG1 transmission time	1 ms
T_{MSG2}	Preamble detection at eNB and MSG2 transmission time	3 ms
T_{MSG3}	Device processing time before sending MSG3	5 ms
$T_{TransMSG3}$	MSG3 transmission time	1 ms
T_{MSG4}	Time of processing MSG3 and sending MSG4	5 ms

number of PDCCH candidates is four. As a result, 12 devices are granted per RAO, and the remainder will again attempt access after a period of time (i.e., T_{MSG2} + RAR_{window} + the time uniformly selected by the device within BO) for a new RAO, unless $Max_{PreamTrans}$ is reached.

For the devices that successfully receive the RAR, they process their RRC connection request (i.e., MSG3) in 5 ms (T_{MSG3}). After that, the devices transmit MSG3 and wait for the RRC connection setup (i.e., MSG4) within 5 ms (T_{MSG4}). The probability of successful delivery is 90% for both MSG3 and MSG4 [9]. The device that fails to deliver MSG3 or receive MSG4 attempts to resend the failure message (i.e., MSG3 or MSG4) with a maximum of five retransmissions ($MaxRetrans_{HARQ}$).

It is assumed that the retransmission of MSG3 and MSG4 is a nonadaptive hybrid automatic repeat request (nonadaptive HARQ). This model was validated against the 3GPP technical report [9] and insignificant differences were found between the two in [13]. Modifications to the system model for adaptation to the proposed approaches are presented in the next subsections.

5.1. PRACH Configuration Index. To consider the PRACH configuration index approach in our system model, we must set the PRACH configuration index to 12. This is accomplished by configuring the RAOs in subframes—0, 2, 4, 6, and 8—where the RAOs increase to reach five RAOs in each frame, as shown in Figure 5(b). As a result, the total number of RAOs for the extreme scenario (over 10 s) is 5,000.

5.2. Pico Cells. To deploy picocells in a macrocell, we must consider different issues. It is important to know where to locate PBS to achieve good coverage extension, the required number of picocells to enhance RACH performance, and the strategy of devices to join PBS. In [36], the authors refer to the importance of increasing the distance between MBS and PBS to improve system performance. Therefore, in our system model, we consider a picocell of a 100 m radius that is placed 750 m away from MBS to achieve good coverage for edge cell devices. Please note that this is a simple assumption to evaluate RACH performance and not an optimum PBS placement, which is beyond the scope of this paper.

In our simulation, we evaluated the RAN performance with 3 and 15 picocells, as shown in Figure 6. Each picocell has its own set of preamble sequences to help reduce collisions (i.e., reducing MSG1 failures). Additionally, each PBS has its own PDCCH resources that increase the number of granted devices. The devices located in the range of the picocell connect through its PBS.

5.3. Aggregation Points. The same assumptions for the picocells are assumed for the aggregation points to enable a consistent comparison between them. Therefore, we follow the picocells scenario by assuming that small networks exist in the same location of the picocells. For those small networks, regardless of their used technology, an aggregation point is placed on the access point. This is used to aggregate device access requests for the devices that are located within the area of the small network. The only condition of the technology used in the small networks is that the coverage of the small cell must support M2M-GW with a good signal quality on the M2M-GW to MBS link. The only difference between them placing PBSs or M2M-GWs is that the M2M-GWs will share the preambles and PDCCH resources with the MBS.

6. RACH Evaluation

The RACH evaluation was conducted with different density values: 5,000, 10,000, 16,000, 20,000, 25,000, and 30,000 [9, 13]. According to the different device density values, we assumed that the devices were uniformly distributed in the range of 50 to 1,000 m from the centre of the macrocell.
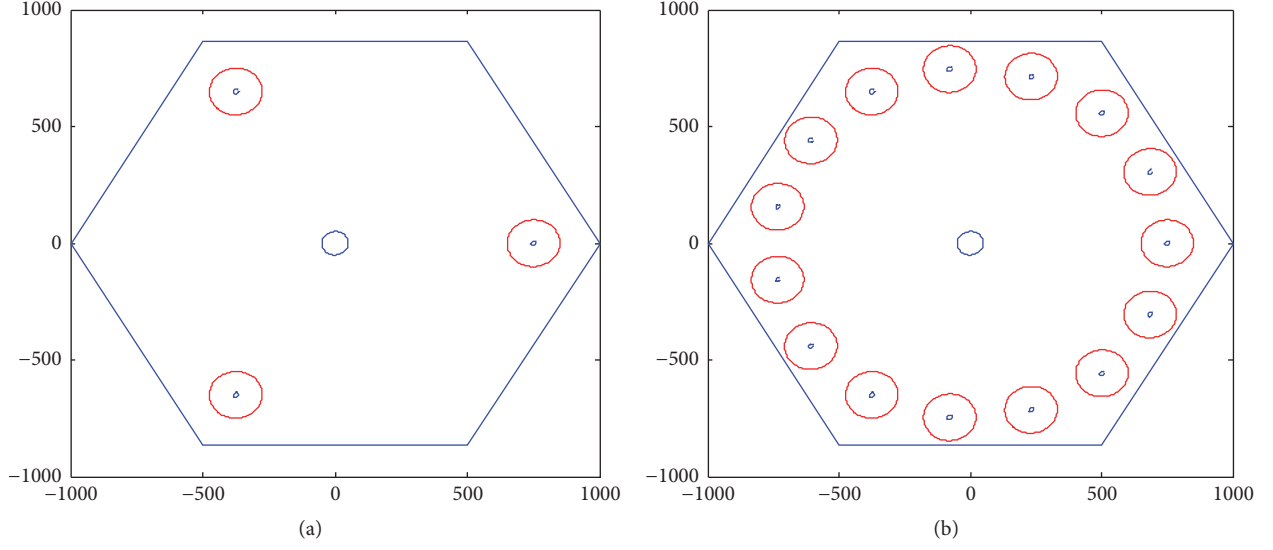
FIGURE 6: Small cell distribution. (a) Three deployed PBSs. (b) Fifteen deployed PBSs.

Owing to the different case studies considered herein, we refer to these cases as follows:

(i) *3GPP-compl. sim.*: 3GPP-compliant simulation that has only one macrocell.

(ii) *PRACH config. index*: 3GPP-compliant simulation with PRACH configuration index 12.

(iii) *3 picocells*: 3GPP-compliant simulation with 3 picocells.

(iv) *15 picocells*: 3GPP-compliant simulation with 15 picocells.

(v) *3 agg. points (1:1)*: 3GPP-compliant simulation with 3 aggregation points (1:1), where the aggregation points act as a tunnel.

(vi) *15 agg. points (1:1)*: 3GPP-compliant simulation with 15 aggregation points (1:1), where the aggregation points act as a tunnel.

(vii) *3 agg. points (1:k)*: 3GPP-compliant simulation with 3 aggregation points (1:k), where the aggregation points aggregate device requests in each RAO.

(viii) *15 agg. points (1:k)*: 3GPP-compliant simulation with 15 aggregation points (1:k), where the aggregation points aggregate device requests in each RAO.

(ix) *3 picocells + PRACH config. index*: 3 picocells combined with PRACH configuration index 12.

(x) *15 picocells + PRACH config. index*: 15 picocells combined with PRACH configuration index 12.

(xi) *3 agg. points (1:1) + PRACH config. index*: 3 aggregation points combined (1:1) with PRACH configuration index 12.

(xii) *15 agg. points (1:1) + PRACH config. index*: 15 aggregation points (1:1) combined with PRACH configuration index 12.
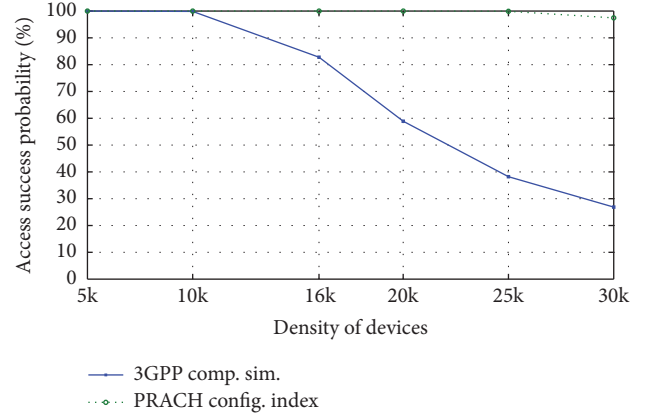

FIGURE 7: Access success probability for 3GPP-compliant simulation versus PRACH configuration index scenario.

(xiii) *3 agg. points (1:k) + PRACH config. index*: 3 aggregation points (1:k) combined with PRACH configuration index 12.

(xiv) *15 agg. points (1:k) + PRACH config. index*: 15 aggregation points (1:k) combined with PRACH configuration index 12.

6.1. RACH Analysis Results. As shown in Figures 7 and 8, it is clear that RACH performance in the PRACH configuration index scenario outperforms RACH performance in the 3GPP-compliant simulation scenario. The increase of RAOs in the PRACH configuration index scenario has a significant effect on the evaluation metrics. The access success probability for most of the density values approaches 100% with at most 48 ms of an average access delay.

In addition, as shown in Figure 9, the average number of preamble transmissions for all density values does not exceed 2.6, which explains the reason behind the reduction
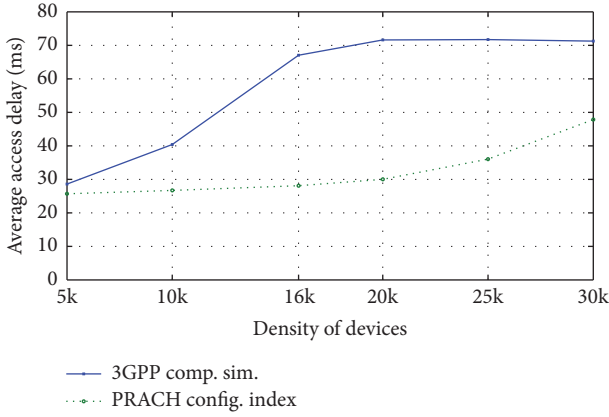
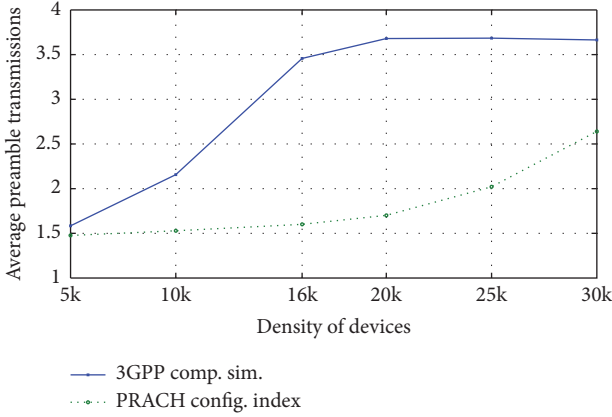FIGURE 8: Average access delay for 3GPP-compliant simulation versus PRACH configuration index scenario.

FIGURE 9: Average preamble transmissions for 3GPP-compliant simulation versus PRACH configuration index scenario.
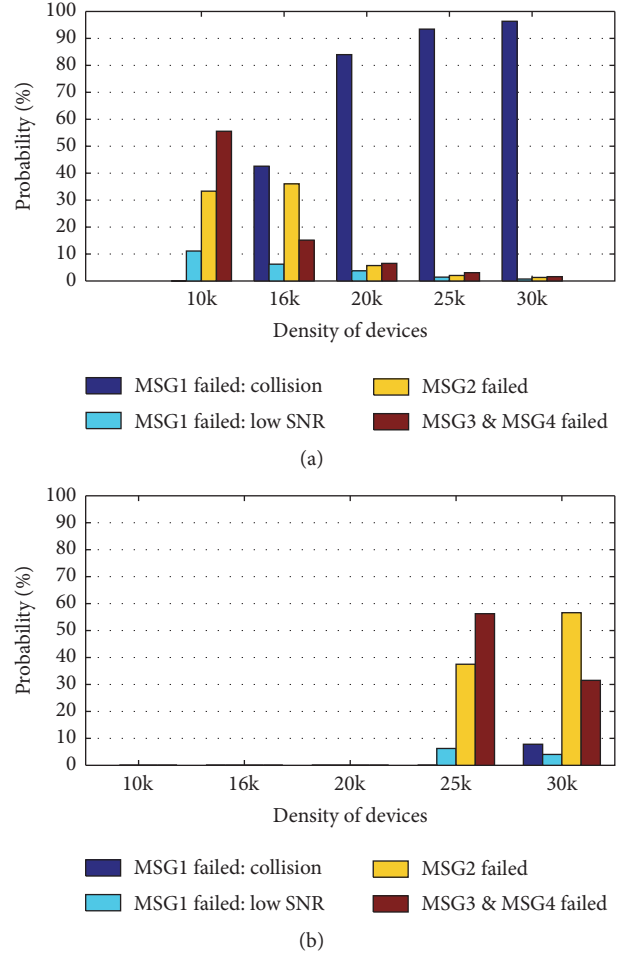

FIGURE 10: Access failure analysis describing the different reasons of access failure. (a) Scenario of 3GPP-compliant simulation. (b) PRACH configuration index scenario.

in the average access delay. Figure 10 illustrates the analysis of the access failure for both scenarios showing the percentage for each reason of the access failure probability. For 5,000 devices, the access success probability in all scenarios is 100%. Therefore, this density value is excluded from the analysis.

In a 3GPP-compliant simulation, for high-density values, the main reason for the RACH failure is the failure of MSG1 because of a preamble collision, as shown in Figure 10(a). For example, in the case of 30,000 devices, the access failure probability is 73.14%. Out of this access failure probability, 96.36% of the devices failed on account of an MSG1 preamble collision, 0.72% are due to MSG1 having a low signal to noise ratio (SNR) because those devices are located on the cell edge, 1.31% are due to MSG2 lacking PDCCH resources, and 1.61% are due to MSG3 and MSG4 failures. MSG3 and MSG4 failed on account of the system model assumption, where the probability of an unsuccessful delivery for both MSG3 and MSG4 is 10%.

For the PRACH configuration index scenario, the only density values with a RACH failure were 25,000 and 30,000 devices, as shown in Figure 10(b). The main reason for the RACH failure in this scenario for the case of 25,000

was the failures of both MSG3 and MSG4. In the case of 30,000 devices, the main reason for the RACH failure was that MSG2 failed on account of the shortage of PDCCH resources. It is furthermore evident in Figure 11 that the collision probability is reduced because there are more RAOs in the PRACH configuration index scenario. We conclude that, by employing the PRACH configuration index scenario, we can achieve a high access success probability with a low average access delay.

In comparing the results of the 3GPP-compliant simulation with the results of the picocell approach in Figure 12, it is obvious that the RACH performance in the picocell approach outperforms the 3GPP-compliant simulation scenario in terms of the access success probability. Referring to Figure 10, the main reason that the access fails in the 3GPP-compliant simulation is the failure of MSG1 on account of the preamble collision. The approaching picocells increase the number of preambles and PDCCH resources. This has an important effect on improving RACH performance. In addition, the role of the picocells to offload the traffic from the macrocell has a significant effect. However, because of the limited coverage
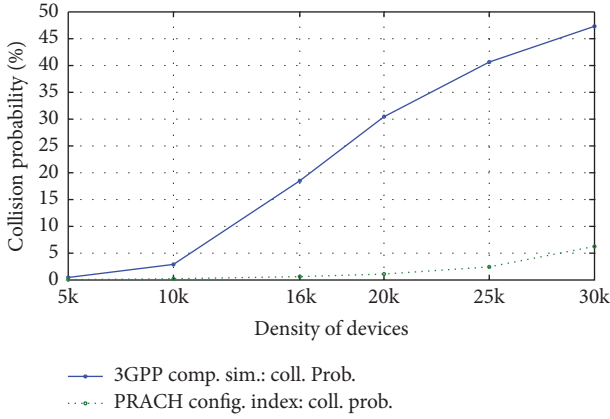
FIGURE 11: Collision probability with respect to RAOs for 3GPP-compliant simulation versus PRACH configuration index scenario.

(a)

(b)

FIGURE 13: Access failure analysis describing the different causes of access failure. (a) Three-picocell scenario. (b) Fifteen-picocell scenario.
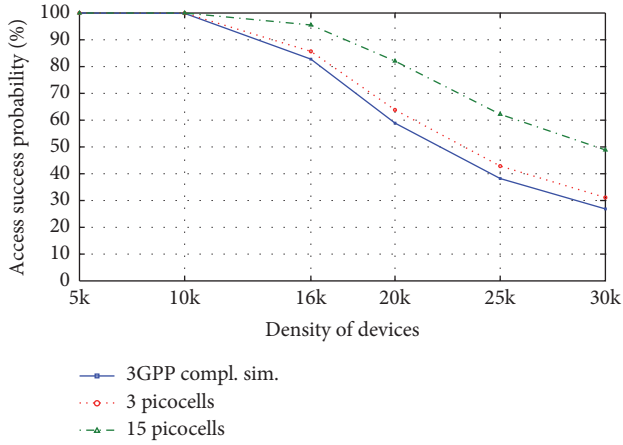

FIGURE 12: Access success probability for 3GPP-compliant simulation versus 3 and 15-picocell scenarios.

of the picocells (i.e., limited in its ability to host a large number of devices because of the assumed picocoverage), not all devices will obtain the benefits of the deployed picocells.

However, the picocell approach improves the RACH performance and increases the access success probability for all ranges of density values in both cases (i.e., 3 and 15 picocells), as shown in Figure 12.

In the three picocells scenario, the increase of the access success probability is small. However, in the 15-picocell scenario, the access success probability is substantially increased compared to the 3GPP-compliant simulation. The analysis of the failure of access for both scenarios is shown in Figure 13. In the three picocells scenario, if the density of devices is less than or equal to 16,000, the access success probability is high. The main reason there is a RACH failure is the lack of PDCCH resources, which can cause an MSG2 failure (three picocells are not adequate).

For the higher density values, the main causes of the access failure are the collisions in MSG1 on account of the high density of devices attempting access in a short period of ti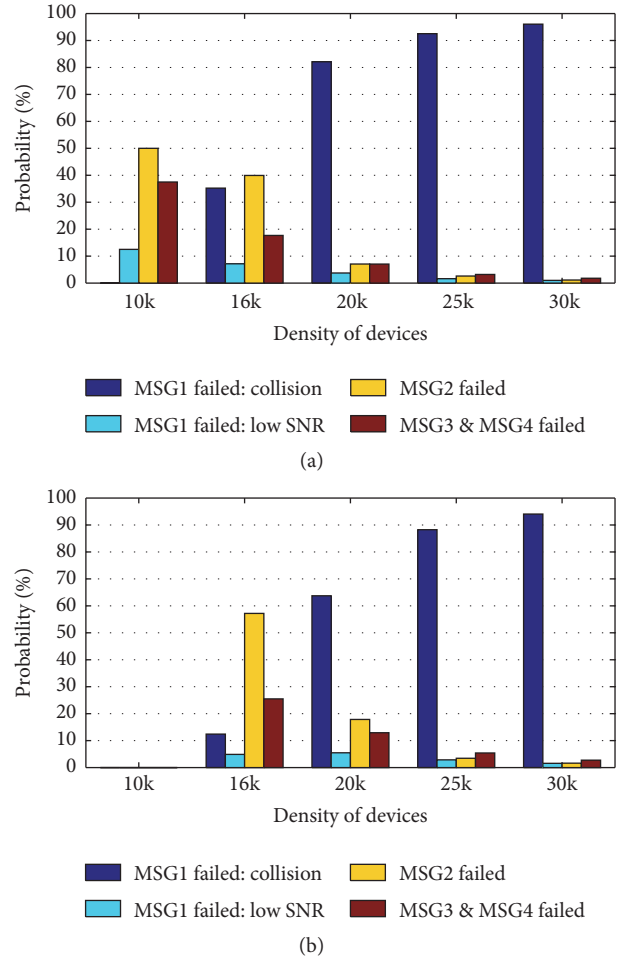me. In the 15-picocell scenario, the access success probability is 100% for the 5,000 and 10,000 cases. For the 16,000 devices, the access failure probability is 4%. The main cause of the RACH failure is again the MSG2 failure on account of the lack of PDCCH resources. However, as the density of devices increases to 30,000 devices, the prime cause of failure is again the collision in MSG1.

In this study, we additionally investigated how the picocell approach affected the average access delay. In this approach, the average access delay was reduced compared to the performance in the 3GPP-compliant simulation, as shown in Figure 14. The same observation was made in terms of the average preamble transmissions, as depicted in Figure 15.

For the scenario of 3 and 15 aggregation points (1:1), the RACH access success probability was similar to that of the 3GPP-compliant simulation, as shown in Figure 16 (the same was observed for the other metrics as well). This result was expected because the role of aggregation points in these scenarios is to pass access devices request to eNB without accumulating requests. We used the mentioned scenarios to verify the implementation of aggregation points in scenarios of 3 and 15 aggregation points (1:k).
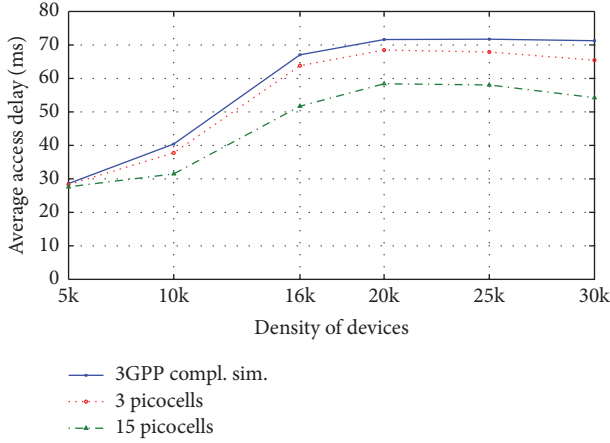
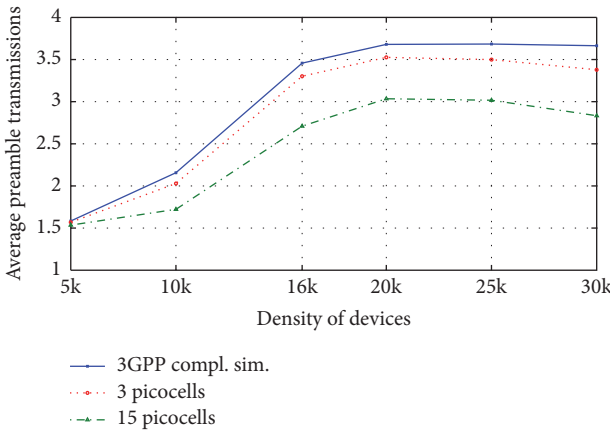Figure 14: Average access delay for the 3GPP-compliant simulation versus 3- and 15-picocell scenarios.

Figure 16: Access success probability for the 3GPP-compliant simulation versus 3 and 15 aggregation points (1:1).

Figure 15: Average preamble transmissions for the 3GPP-compliant simulation versus 3- and 15-picocell scenarios.

Figure 17: Access success probability for the 3GPP-compliant simulation versus 3 and 15 aggregation points (1:k).

In the aggregation point approach, the aggregation point collected or aggregated the request of the devices in each RAO (i.e., 3- and 15-aggregation-point (1:k) scenarios). The results showed a slight improvement in terms of access success probability only in the scenario of 15 aggregation points (1:k) (Figure 17). This was the case because of the very small reduction of the collision probability since the role of the aggregation point is to group the device requests in the same RAO and send them as one request. This causes a slight reduction in the average number of preamble transmissions.

However, it is important to note that the aggregation points did not perform as well because of the small amount of aggregated requests and owing to the traffic pattern, where the arrival of devices followed a beta distribution (i.e., a maximum of four requests). The remaining results of the 3- and 15-aggregation point (1:k) scenarios were similar to those of the 3GPP-compliant simulation. Thus, the figures are not included.

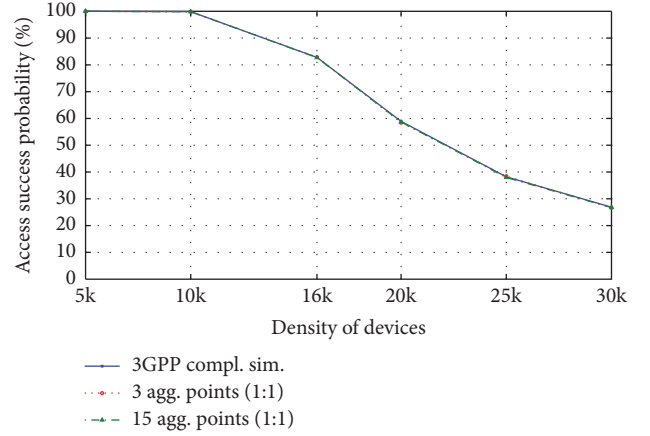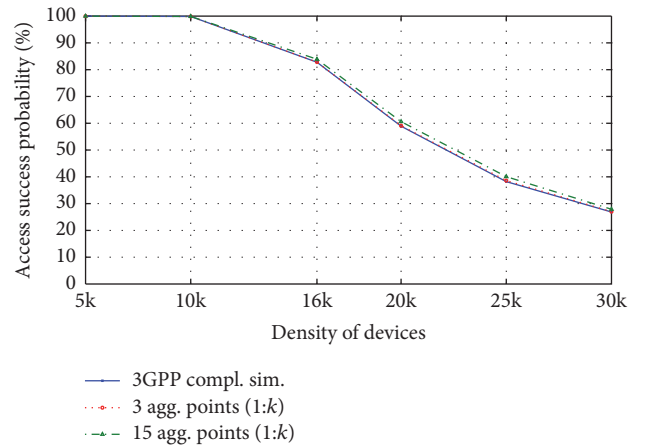The analysis of RACH failure for scenarios of 3 and 15 aggregation points (1:k) was slightly different compared to the analysis in the 3GPP-compliant simulation (Figure 18). For 10,000 devices, the probability of access failure was very low. For the case of 16,000 devices, the cause of the RACH failure was the failure of MSG2. This was different from the analysis of the failure in the 3GPP-compliant simulation scenario, where the high percentage of RACH failures was because of collisions. For the high-density values, the main causes of the RACH failure were the collisions, as in the 3GPP-compliant simulation. In the scenarios of 3 and 15 aggregation points (1:k), the failure due to collisions decreased compared to that of the 3GPP-compliant simulation. However, this resulted in an increase in the contention of the devices on the eNB requesting PDCCH resources, which led to the MSG2 failure.

In this study, we additionally evaluated a combination of the proposed methods (the PRACH configuration index scenario combined with picocell and aggregation point approaches) (Table 2). The table includes the numerical results of the 3GPP-compliant simulation and the PRACH configuration index scenarios for a comparison with the previously discussed results for the latter scenarios.
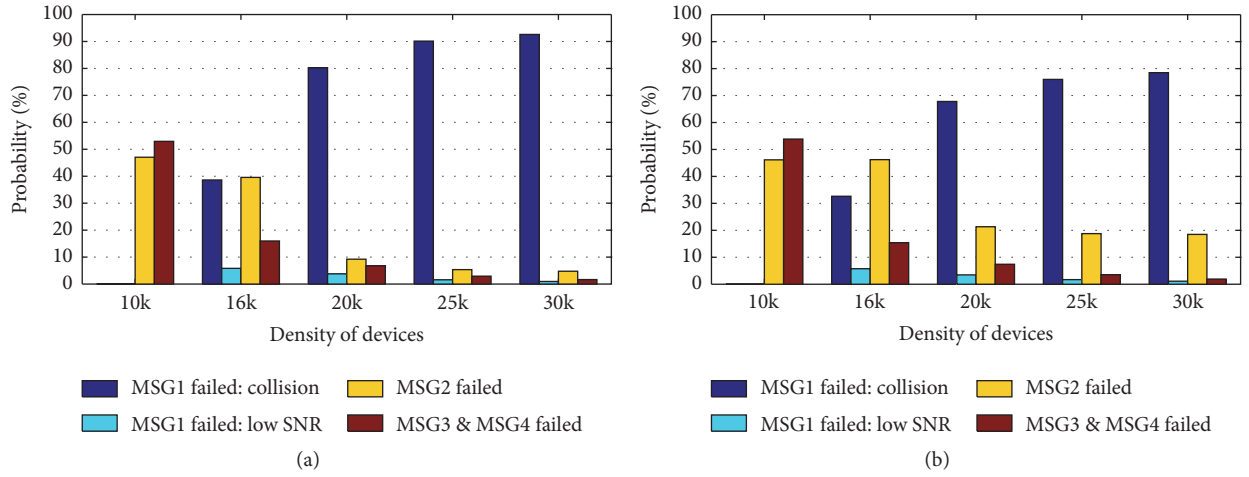
FIGURE 18: Access failure analysis describing the different causes of access failure. (a) Three-aggregation-point (1:k) scenario. (b) Fifteen-aggregation-point (1:k) scenario.

TABLE 2: RACH performance for 3GPP-compliant simulation and the proposed solutions.

Evaluation metrics	M	3GPP compl. sim.	PRACH config. index	3 picocells + PRACH config. index	15 picocells + PRACH config. index	3 agg. points (1:1) + PRACH config. index	15 agg. points (1:1) + PRACH config. index	3 agg. points (1:k) + PRACH config. index	15 agg. points (1:k) + PRACH config. index
	5k	100	100	100	100	100	100	100	100
	10k	99.86	100	100	100	100	100	100	100
Access success	16k	82.78	100	100	100	100	100	100	100
probability (%)	20k	58.90	100	100	100	100	100	100	100
	25k	38.21	99.91	99.95	100	99.92	99.91	99.91	99.92
	30k	26.86	97.44	98.53	99.94	97.39	97.41	97.51	97.69
	5k	28.61	25.70	25.49	25.2	25.55	25.49	25.36	25.73
	10k	40.41	26.71	26.44	25.87	26.62	26.61	26.77	26.56
Average access	16k	67.05	28.11	27.85	26.79	27.9	28	27.85	27.89
delay (ms)	20k	71.62	30.01	29.29	27.61	30.18	30.07	29.9	29.91
	25k	71.71	36.05	34.36	29.41	35.75	35.92	36.05	35.64
	30k	71.26	47.86	44.39	33.47	47.76	47.68	47.55	47.27
	5k	1.58	1.48	1.46	1.45	1.47	1.47	1.46	1.48
	10k	2.16	1.53	1.51	1.48	1.52	1.52	1.53	1.52
Average number	16k	3.46	1.60	1.59	1.53	1.59	1.6	1.59	1.58
of preamble	20k	3.68	1.70	1.67	1.58	1.71	1.71	1.7	1.69
transmissions	25k	3.68	2.02	1.93	1.67	2	2.01	2.02	1.98
	30k	3.66	2.64	2.46	1.89	2.64	2.63	2.62	2.59

In the combined approach of the picocell and PRACH configuration index, the advantage of the PRACH configuration index approach (i.e., the increase of the RAOs) supplements the advantages of the picocell approach (i.e., additional preambles and the offloading feature). As evident in Table 2, the results for this scenario outperform the results of all the previous scenarios for access success probability, average access delay, and average preamble transmissions. Note that, by following the combined approaches of the PRACH configuration index and picocells, the access success probability is approximately 100% for all density values,

except for the 30,000 devices, in the case of using three picocells in the combined picocell and PRACH configuration index approach.

For the remaining scenarios, in which the PRACH configuration index is combined with the aggregation point approach, the RACH performance shown in Table 2 is similar to the performance of scenario two, as expected from the previous results.

A comparison of the best results of RACH performance for the proposed schemes in [9, 14, 15, 23] that considers traffic model two with 30,000 devices and select methods of the

TABLE 3: Comparison results of proposed and existing methods.

Scheme	Access success prob. (%)	Avg. access delay (ms)	Avg. preamble trans.
Longer backoff scheme (max. 960) [14]	100	—	1.86
Prebackoff scheme (max. 960) [14]	100	—	1.51
ACB [14]:			
M2M ACB factor = 0.5	68.98	—	—
ACB time = 16			
Separate RACH resources [14]:	11.46	—	—
M2M/UE is 53/1			
Dynamic allocation of RACH resources [14]:			
100% additional	21.26	—	—
subframes for M2M			
dedicated access			
PRA [15]	93.9	2937	—
Some methods proposed in this work			
PRACH config. index	97.44	47.86	2.64
15 picocells	48.88	54.25	2.83
15 agg. points (1:k)	27.89	71.10	3.60
15 picocells + PRACH config. index	99.94	33.47	1.89
15 agg. points (1:k) + PRACH config. index	97.69	47.27	2.59

proposed schemes of this work are presented in Table 3. As shown in the table, the longer backoff scheme and prebackoff scheme proposed in [14] have the highest access success probability and low average preamble transmissions compared to the other schemes. However, there are no numerical results for the access delay because those schemes are only proposed to solve RAN congestion for delay-tolerant devices. In this study, our approaches (i.e., PRACH configuration index, 15 picocells with the PRACH configuration index, and 15 aggregation points with the PRACH configuration index) can serve different M2M applications with an acceptable average access delay, high access success probability, and low average preamble transmissions.

6.2. Discussion. Our results show that the PRACH configuration index approach substantially improves RACH performance of access success probability, average access delay, average preamble transmissions, and collision probability on account of the increase of the RAOs. This approach is suitable for nondelay tolerant M2M applications because of its advantages. On the other hand, because the RA procedure uses six resource blocks in each subframe, 12.5% of the uplink

resources in a 5 MHz bandwidth are consumed once the PRACH configuration index is set to 12 [9]. Nevertheless, we believe this approach can be used without sacrificing the service quality of the upload transmission, especially if we switch to a higher bandwidth (e.g., 20 MHz, where the number of resource blocks is 100) because most of the M2M applications consider small data transmissions. This approach is applicable to general M2M service requirements, such as subscription management, adding or removing M2M characteristics, or controlling traffic. In this approach, the network operator controls MBS, which, in turn, manages the cellular M2M-Ds.

The picocell approach performs well, particularly in terms of access success probability, average access delay, and average preamble transmissions for all density values if the number of deployed picocells is increased. This result is on account of the increased number of preambles, availability of PDCCH resources, and reduced traffic on eNB, which can effectively improve congestion and enhance RACH performance. However, there is an associated cost with introducing additional picocells. This approach is applicable to general M2M service requirements because PBS is likewise controlled by the network operator.

Deploying a large number of aggregator points to collect device requests in M2M architecture does not considerably enhance RACH performance in this scenario.

As expected in the combination approaches, RACH performance is improved. In our analysis, the most promising solution that achieves high access success probability, low average access delay, and low average preamble transmissions is the case of 15 picocells combined with the PRACH configuration index.

7. Conclusions

This paper provides an analysis of the RA procedure for M2M communications over LTE-A. The focus of this study was an extreme scenario with a heavy density of devices attempting to access the network in a short period of time and in a synchronized manner. In this paper, we proposed three methods to improve RACH capacity performance. The PRACH configuration index approach achieved a significant improvement in RACH performance for all cases including a massive number of devices in terms of access success probability, average access delay, and average preamble transmissions.

A significant reduction in the collision probability compared to the 3GPP-compliant simulation was additionally determined. The picocell approach with 15 picocells enhanced RACH performance in terms of access success probability, average access delay, and average number of preamble transmissions. For the case of aggregation points, only a very slight enhancement was observed for the number of aggregation points investigated. The method that combined the PRACH configuration index with picocells performed better than all methods. In short, deploying any of the mentioned approaches depends on different issues, such as the type of M2M application and deployment costs.

Competing Interests

The authors declare that there is no conflict of interests regarding the publication of this paper.

Acknowledgments

References

[1] ETSI TS 102 690 V2.1.1, "Machine-to-Machine Communications (M2M): Functional Architecture," October 2013.

[2] ETSI TS 102 689 V1.1.1, "Machine-to-Machine Communications (M2M): M2M Service Requirements," August 2010.

[3] 3GPP TR 23.888 V11.0.0, "System Improvements for Machine-Type Communications (MTC)," September 2012.

[4] 3GPP TS 22.368 V13.1.0, "Service Requirements for Machine-Type Communications (MTC); Stage 1," December 2014.

[5] K. Zheng, F. L. Hu, W. B. Wang, W. Xiang, and M. Dohler, "Radio resource allocation in LTE-advanced cellular networks with M2M communications," *IEEE Communications Magazine*, vol. 50, no. 7, pp. 184–192, 2012.

[6] "Standardization of Machine-type Communications, V0.2.4," June 2014.

[7] Cisco Visual Networking Index, "Cisco visual networking index: global mobile data traffic forecast update, 2014–2019," White Paper, 2015, http://www.cisco.com/c/en/us/solutions/collateral/service-provider/visual-networking-index-vni/white_paper_c11-520862.html.

[8] 3GPP TSG RP-141865, "Revised WI: Further LTE Physical Layer Enhancements for MTC," RAN Meeting no. 66, Ericsson, Edinburgh, Scotland, September 2014.

[9] 3GPP TR 37.868 V11.0.0, "Study on RAN Improvements for Machine-type Communications," September 2011.

[10] H. Shariatmadari, R. Ratasuk, S. Iraji et al., "Machine-type communications: current status and future perspectives toward 5G systems," *IEEE Communications Magazine*, vol. 53, no. 9, pp. 10–17, 2015.

[11] 3GPP TSG R2-112198, "Clarification on the Discussion of RACH Collision Probability," ITRI 3GPP TSG-RAN WG2 Meeting no. 73b, Shanghai, China, April 2011.

[12] R.-G. Cheng, C.-H. Wei, S.-L. Tsao, and F.-C. Ren, "RACH collision probability for machine-type communications," in *Proceedings of the IEEE 75th Vehicular Technology Conference (VTC '12)*, pp. 1–5, IEEE, Yokohama, Japan, June 2012.

[13] F. Alsewaidi, D. Kaleshi, and A. Doufexi, "Analysis of radio access network performance for M2M communications in LTE-A at 800 MHz," in *Proceedings of the IEEE Wireless Communications and Networking Conference Workshops (WCNCW '14)*, pp. 110–115, Istanbul, Turkey, April 2014.

[14] 3GPP TSG R2-112863, "Backoff Enhancements for RAN Overload Control," 3GPP TSG RAN WG2 no. 73bis, Barcelona, Spain, May 2011.

[15] J.-P. Cheng, C.-H. Lee, and T.-M. Lin, "Prioritized Random Access with dynamic access barring for RAN overload in 3GPP LTE-a networks," in *Proceedings of the IEEE GLOBECOM Workshops (GC Wkshps '11)*, pp. 368–372, December 2011.

[16] S.-Y. Lien, K.-C. Chen, and Y. Lin, "Toward ubiquitous massive accesses in 3GPP machine-to-machine communications," *IEEE Communications Magazine*, vol. 49, no. 4, pp. 66–74, 2011.

[17] M.-Y. Cheng, G.-Y. Lin, H.-Y. Wei, and A. C.-C. Hsu, "Overload control for machine-type-communications in LTE-advanced system," *IEEE Communications Magazine*, vol. 50, no. 6, pp. 38–45, 2012.

[18] A. Laya, L. Alonso, and J. Alonso-Zarate, "Is the random access channel of LTE and LTE-A suitable for M2M communications? A survey of alternatives," *IEEE Communications Surveys & Tutorials*, vol. 16, no. 1, pp. 4–16, 2014.

[19] M. Hasan, E. Hossain, and D. Niyato, "Random access for machine-to-machine communication in LTE-advanced networks: issues and approaches," *IEEE Communications Magazine*, vol. 51, no. 6, pp. 86–93, 2013.

[20] M.-Y. Cheng, G.-Y. Lin, H.-Y. Wei, and C.-C. Hsu, "Performance evaluation of radio access network overloading from machine type communications in LTE—a networks," in *Proceedings of the IEEE Wireless Communications and Networking Conference Workshops (WCNCW '12)*, pp. 248–252, April 2012.

[21] C.-Y. Oh, D. Hwang, and T.-J. Lee, "Joint access control and resource allocation for concurrent and massive access of M2M devices," *IEEE Transactions on Wireless Communications*, vol. 14, no. 8, pp. 4182–4192, 2015.

[22] F. Ghavimi and H.-H. Chen, "M2M communications in 3GPP LTE/LTE-A networks: architectures, service requirements, challenges, and applications," *IEEE Communications Surveys & Tutorials*, vol. 17, no. 2, pp. 525–549, 2015.

[23] 3GPP TSG R2-104662, "MTC Simulation Results with Specific Solutions," RAN WG2 no. 71, Madrid, Spain, August 2010.

[24] J. S. Vardakas, N. Zorba, C. Skianis, and C. V. Verikoukis, "Performance analysis of M2M communication networks for QoS-differentiated smart grid applications," in *Proceedings of the IEEE Globecom Workshops (GC Wkshps '15)*, pp. 1–6, IEEE, San Diego, Calif, USA, December 2015.

[25] G.-Y. Lin, S.-R. Chang, and H.-Y. Wei, "Estimation and adaptation for bursty LTE random access," *IEEE Transactions on Vehicular Technology*, vol. 65, no. 4, pp. 2560–2577, 2016.

[26] Y. Chang, C. Zhou, and O. Bulakci, "Coordinated random access management for network overload avoidance in cellular machine-to-machine communications," in *Proceedings of the European Wireless, 20th European Wireless Conference*, pp. 1–6, Barcelona, Spain, 2014.

[27] S.-Y. Lien, T.-H. Liau, C.-Y. Kao, and K.-C. Chen, "Cooperative access class barring for machine-to-machine communications," *IEEE Transactions on Wireless Communications*, vol. 11, no. 1, pp. 27–32, 2012.

[28] G. Foddis, R. G. Garroppo, S. Giordano, G. Procissi, S. Roma, and S. Topazzi, "On RACH preambles separation between human and machine type communication," in *Proceedings of the IEEE International Conference on Communications (ICC '16)*, Kuala Lumpur, Malaysia, 2016.

[29] F. Alsewaidi, D. Kaleshi, and A. Doufexi, "Performance comparison of LTE-A RAN operating in 800MHz and 2.4GHz bands for M2M communications," in *Proceedings of the 11th International Symposium on Wireless Communications Systems (ISWCS '14)*, pp. 824–829, Barcelona, Spain, August 2014.

[30] R. Ratasuk, A. Prasad, Z. Li, A. Ghosh, and M. Uusitalo, "Recent advancements in M2M communications in 4G networks and evolution towards 5G," in *Proceedings of the 18th International Conference on Intelligence in Next Generation Networks (ICIN '15)*, pp. 52–57, IEEE, Paris, France, February 2015.

[31] S.-P. Yeh, S. Talwar, G. Wu, N. Himayat, and K. Johnsson, "Capacity and coverage enhancement in heterogeneous networks," *IEEE Wireless Communications*, vol. 18, no. 3, pp. 32–38, 2011.

[32] P. Popovski, G. Mange, A. Roos et al., "Deliverable D6. 3 intermediate system evaluation results," ICT 317669, METIS, 2014.

[33] G. Wu, S. Talwar, K. Johnsson, N. Himayat, and K. D. Johnson, "M2M: from mobile to embedded internet," *IEEE Communications Magazine*, vol. 49, no. 4, pp. 36–43, 2011.

[34] A. Lo, Y. W. Law, and M. Jacobsson, "A cellular-centric service architecture for machine-to-machine (M2M) communications," *IEEE Wireless Communications*, vol. 20, no. 5, pp. 143–151, 2013.

[35] C. W. Johnson, *Long Term Evolution in Bullets*, Northampton, England, UK, 2012.

[36] P. Tian, H. Tian, L. Gao, J. Wang, X. She, and L. Chen, "Deployment analysis and optimization of Macro-Pico heterogeneous networks in LTE-A system," in *Proceedings of the 15th International Symposium on Wireless Personal Multimedia Communications (WPMC '12)*, pp. 246–250, September 2012.